



CHORUS

This is the accepted manuscript made available via CHORUS. The article has been published as:

Unraveling Photoinduced Spin Dynamics in the Topological Insulator Bi_2Se_3

M. C. Wang, S. Qiao, Z. Jiang, S. N. Luo, and J. Qi

Phys. Rev. Lett. **116**, 036601 — Published 22 January 2016

DOI: [10.1103/PhysRevLett.116.036601](https://doi.org/10.1103/PhysRevLett.116.036601)

Unraveling photoinduced spin dynamics in topological insulator Bi_2Se_3

M. C. Wang,^{1,2} S. Qiao,^{3,4} Z. Jiang,⁵ S. N. Luo,^{1,2} and J. Qi^{1,2,*}

¹*The Peac Institute of Multiscale Sciences, Chengdu, Sichuan 610031, P. R. China*

²*Key Laboratory of Advanced Technologies of Materials, Ministry of Education, Southwest Jiaotong University, Chengdu, Sichuan 610031, P. R. China*

³*State Key Laboratory of Functional Materials for Informatics, Shanghai Institute of Microsystem and Information Technology,*

Chinese Academy of Sciences, Shanghai, Shanghai 200050, P. R. China

⁴*School of Physical Science and Technology, ShanghaiTech University, Shanghai 200031, P. R. China*

⁵*School of Physics, Georgia Institute of Technology, Atlanta, Georgia 30332, USA*

(Dated: January 5, 2016)

We report on time-resolved ultrafast optical spectroscopy study of the topological insulator (TI) Bi_2Se_3 . We unravel that a net spin polarization can not only be generated using circularly polarized light via interband transitions between topological surface states (SSs), but also via transitions between SSs and bulk states. Our experiment demonstrates that tuning photon energy or temperature can essentially allow for photoexcitation of spin-polarized electrons to unoccupied topological SSs with two distinct spin relaxation times (~ 25 fs and ~ 300 fs), depending on the coupling between SSs and bulk states. The intrinsic mechanism leading to such distinctive spin dynamics is the scattering in SSs and bulk states which is dominated by E_g^2 and A_{1g}^1 phonon modes, respectively. These findings are suggestive of novel ways to manipulate the photoinduced coherent spins in TIs.

PACS numbers: 03.65.Vf, 72.25.Fe, 72.25.Rb, 78.47.J, 78.68.+m

Topological insulators (TIs), as a new quantum phase of matter, are characterized by an unusual electronic structure exhibiting both insulating bulk and robust metallic surface states (SSs) [1, 2]. This unique electronic structure combining external light excitation on TIs leads to many exotic physical phenomena [3–12], which hold TIs a great promise for opto-spintronics and ultrafast spintronics applications [13]. Therefore, it becomes crucial to study the out-of-equilibrium properties of TIs under photo-excitation. Among them, the charge and spin dynamics have attracted a lot of recent attention, and are explored effectively using the time- and angle-resolved photoemission spectroscopy (Tr-ARPES) [14–21] and time-resolved optical spectroscopy [22–32]. Investigation of the non-equilibrium charge dynamics enables deep understanding of the momentum scattering, which is a fundamental process determining the electronic transport in TIs [33]. On the other hand, comprehensive knowledge of the spin dynamics, including coherent spin generation and relaxation, is vital for actively manipulating spins in spintronics [34]. Most of previous time-resolved works focus on the charge dynamics in TIs, and have revealed that the electron-phonon (e-p) coupling plays a key role in momentum scattering of the non-equilibrium carriers. In contrast, very few works pay attention on the photoinduced coherent spin dynamics in TIs [24, 35, 36]. Specifically, several key questions are still open regarding the dynamical response of the spin properties to the incident light: (1) Can a surface net spin polarization be generated via interband transitions from bulk states to SSs using circularly polarized light? (2) Does the spin dynamics in topological SSs and bulk states behave in a similar manner? Or does the same

mechanism dictate the spin dynamics in topological SSs and bulk states?

In this Letter, we employ time-resolved transient reflectivity and Kerr rotation measurements to investigate the photo-excited charge and coherent spin dynamics in the prototypical TI Bi_2Se_3 . Two types of helicity-dependent photoinduced net spin polarization have been unveiled, and can be attributed to the interband transitions between SSs and bulks and between SSs and SSs, respectively. We show that two coherent spin dynamics with distinct spin relaxation times can be selectively excited by tuning the photon energy $h\nu$ or temperature T . We reveal that the e-p scattering in SSs and bulk states dominated by different phonon modes gives rise to the distinct spin relaxation.

Time-resolved transient reflectivity change $\Delta R(t)/R$ and time-resolved Kerr rotation (TRKR) $\Delta\theta_K(t)$ were measured based on a pump-probe scheme using a Ti:sapphire laser with a time resolution of ~ 35 fs. Experiments were performed on high quality Bi_2Se_3 samples with carrier density $n \simeq 4 \times 10^{18} \text{ cm}^{-3}$. The Fermi level E_f resides inside the bulk band-gap, and is ~ 0.1 eV above the Dirac point. Detailed description of the materials and the measurement setup can be found in Supplemental Material [37].

Figure 1(a) shows a typical transient reflectivity $\Delta R/R$ signal, where an initial fast-decaying component is followed by slow relaxation processes superimposed with an oscillatory behavior. An exponential fit to the initial fast decay (blue line) exhibits a time constant of $\tau_{ep} \simeq 300$ fs, consistent with the cooling time of electrons in the bulk bands for electronic temperature $T_e \gtrsim 600$ K [14, 15]. Since in such a state the optical phonon cooling

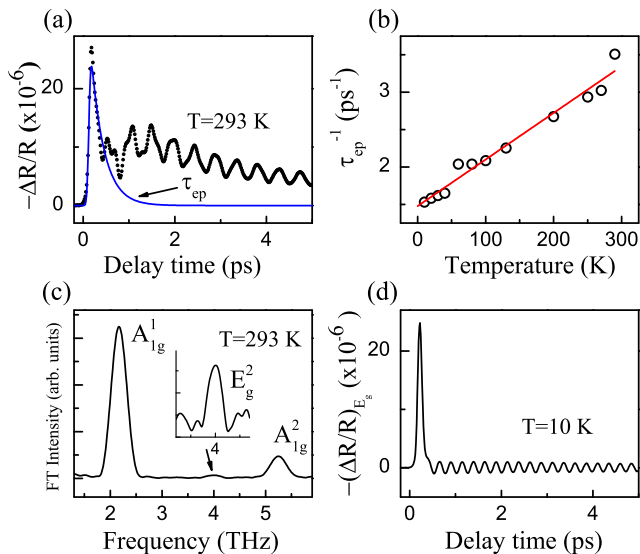


FIG. 1. (a) Typical $\Delta R/R$ measurement on Bi_2Se_3 at 293 K with $h\nu \sim 1.55$ eV. The blue line is an exponential fit to the initial fast decay. (b) Electron-phonon scattering rate τ_{ep}^{-1} as a function of temperature. The red line is a linear fit. (c) Fourier transform (FT) spectra of the oscillatory behaviour. (d) Typical $(\Delta R/R)_{E_g}$ signal associated with the E_g phonon modes at 10 K.

is expected to be the most effective channel, the fast-decaying component can be attributed to an electron-optical-phonon scattering process. The corresponding scattering rate τ_{ep}^{-1} as a function of T ($T \gtrsim 10$ K) is shown in Fig. 1(b), where the linear-in- T behavior is expected for a given Debye temperature of $\Theta_D \sim 180$ K [28]. The following slow relaxation has a time constant of ~ 1 ps, in well agreement with previous findings of the electron-phonon scattering time associated with the low energy phonons [14–17, 22–24, 32]. We can extract the oscillatory component in $\Delta R/R$, whose Fourier transform (FT) reveals several frequencies [as shown in Fig. 1(c)], e.g., ~ 2.2 THz, 4 THz, and 5.2 THz at 293 K. These terahertz oscillations are due to coherent optical phonons, initiated via either coherent Raman scattering [38] or dispersive excitation [39]. The three peaks in Fig. 1(c) from left to right are attributed to A_{1g}^1 , E_g^2 , and A_{1g}^2 Raman-active optical phonon modes, respectively [40]. Another E_g^1 Raman-active mode can also be observed at low temperatures (see Supplemental Material [37]). Among all the optical phonon modes, A_{1g}^1 is the strongest, suggesting that electron- A_{1g}^1 -optical-phonon coupling dominates the e-p scattering or the momentum scattering time (τ_p) in the excited bulk states within the initial ~ 500 fs, as also indicated by the Tr-ARPES measurements [20].

In addition, one can unambiguously extract component $(\Delta R/R)_{E_g}$ from $\Delta R/R$ [Fig. 1(d)], which directly shows the electron-phonon scattering process coupled solely with the E_g phonon modes (E_g^2 dominates, see Supplemental Material [37]). Fitting $(\Delta R/R)_{E_g}$ with an

exponential decay, we obtain an electron-phonon scattering time of $\tau_{ep}^* \simeq 30$ fs, which is nearly temperature independent. Clearly, τ_{ep}^* is about 10 times faster than τ_{ep} associated with the dominant A_{1g}^1 phonon mode. Our experiment thus evidently demonstrates that scattering events coupled with different phonon modes will decay in distinct timescales.

Figure 2(a) shows typical measurements of $\Delta\theta_K$ at low and high temperatures. It can be seen that the circularly polarized light generates a non-equilibrium net spin polarization in Bi_2Se_3 , as the Kerr rotation signals change sign with the helicity of the pump light. This observation is consistent with that reported in Ref. [24], where the spin relaxation time is ~ 200 fs (limited by time-resolution) for excited electrons in either SSs or bulk states of Bi_2Se_3 at room temperature. In this work, our TRKR signals evidently reveal novel complex structures.

Microscopically, generation of a net spin density in opaque materials by circularly polarized light involves direct optical transitions between different energy levels and the accompanying angular momentum transfer (spin selection rules), as in GaAs [41]. Therefore, in order to understand the nature of the related electronic states, we have carried out detailed measurements on the $h\nu$ -dependent and T -dependent $\Delta\theta_K$. The results are shown in Figs. 2(a)-(c). Here, we first notice that the $h\nu$ -dependence of $\Delta\theta_K$ resembles the T -dependence. This similarity can be understood by the band-gap shrinkage (BGS) with increasing T via electron-phonon interactions commonly seen in most semiconductors [42]. Due to the BGS effect, the influence on optical transitions by increasing T is analogous to that by increasing $h\nu$.

From Figs. 2(a)-(c), we also find that three dynamical processes contribute to $\Delta\theta_K(t)$. An ultrafast transient with positive sign (indicated by green arrows) dominates at large $h\nu$ or high T , but almost disappears at small $h\nu$ or low T . It lasts for about 100 fs. A relatively slow decay component with negative sign (indicated by blue arrows) is observed at all investigated $h\nu$ and T . It is persistent to ~ 1.2 ps. The third process with positive sign (indicated by magenta arrows) appears at small $h\nu$ and low T . It also lasts for about 1.2 ps. Quantitatively, these three processes can be fitted using three exponential decays with time constants τ_s , τ_b , and τ_{sb} , respectively. The fitted results agree well with the experimental data [Fig. 2(c)]. Similar data have also been obtained in highly n -doped samples (see Supplemental Material [37]).

According to the previous Tr-ARPES studies [18, 19], the instantaneous populated states from the optical transitions with $h\nu \sim 1.61$ eV should involve the second topological SS (SS_2) above the bulk conduction band (BCB_1), as shown in Fig. 3. In this situation, the allowable direct optical transitions are from the first topological SS (SS_1) to SS_2 , from the first bulk valence band (BVB_1) to the second high-lying bulk valence band (BVB_2), and from SS_1 to BVB_2 [Fig. 3(a)]. These transitions are symbol-

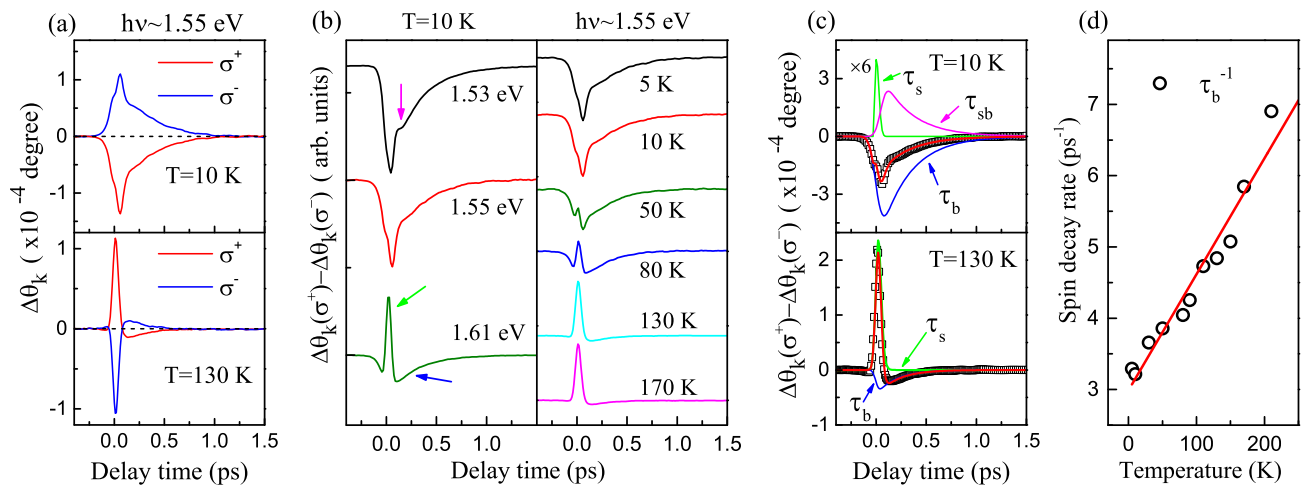


FIG. 2. (a) Time-resolved Kerr rotation, $\Delta\theta_K$, induced by left (σ^+) and right (σ^-) circularly polarized light at 10 K and 130 K. (b) Excitation photon energy ($h\nu$) and temperature (T) dependence of $[\Delta\theta_K(\sigma^+) - \Delta\theta_K(\sigma^-)]$, where $\Delta\theta_K(\sigma^+) - \Delta\theta_K(\sigma^-) \simeq 2\Delta\theta_K(\sigma^+)$. (c) Exponential decay fittings (red lines) for experimental $\Delta\theta_K$ at 10 K and 130 K with $h\nu \sim 1.55$ eV (black squares). Green, magenta, and blue lines describe three distinct dynamical processes characterized by τ_s , τ_{sb} , and τ_b , respectively. (d) Spin decay rate τ_b^{-1} as a function of T . The red line is a linear fit.

ized by $SS_1 \rightarrow SS_2$, $BVB_1 \rightarrow BVB_2$, and $SS_1 \rightarrow BVB_2$, respectively. However, when $h\nu$ or T is relatively small, $h\nu$ becomes insufficient for populating SS_2 via $SS_1 \rightarrow SS_2$, although $BVB_1 \rightarrow BVB_2$ and $SS_1 \rightarrow BVB_2$ can still occur. Apparently, if the process characterized by τ_s is attributed to the relaxation of the spin-polarized electrons in SS_2 via $SS_1 \rightarrow SS_2$, the corresponding TRKR signal should vanish with decreasing $h\nu$ or T , in well consistent with our experimental observations [Fig. 2]. This scenario is also consistent with the theoretical works of Refs. [9, 10], that is, the spin-polarized electrons can be generated by SS-to-SS interband transitions with particular spin selection rules using circularly polarized light.

The spin dynamics characterized by τ_b occurs at all $h\nu$ and T investigated, where both transitions $BVB_1 \rightarrow BVB_2$ and $SS_1 \rightarrow BVB_2$ are always allowed [Fig. 3]. However, the electrons excited by σ^\pm photons via interband transitions between bulk states should be essentially unpolarized, due to the bulk inversion symmetry [35]. Even if for some other reasons, a net spin polarization is generated from the transition between bulk states $BVB_1 \rightarrow BVB_2$, it is expected to be $h\nu$ - and T -independent, as the total number of the populated bulk states remains nearly intact in the energy range investigated [Figs. 3(a) and (b)]. But, experimentally, we find that the amplitude of τ_b process exhibits a strong $h\nu$ and T -dependence: it decreases with increasing $h\nu$ and T , as shown in Figs. 2(b) and (c). Such dependence is consistent with the population change associated with $SS_1 \rightarrow BVB_2$. Therefore, one can naturally attribute τ_b to the spin relaxation of excited electrons in BVB_2 , as illustrated in Figs. 3(c) and (d). It is worth noting that, due to angular momentum conservation, the spin-polarized electrons in bulk states excited from SSs should have

an opposite polarization direction to that in SSs excited from bulk states. This phenomenon is indeed observed in highly n -doped samples, where additional transition $BCB_1 \rightarrow SS_2$ induces a surface net spin polarization in SS_2 opposite to the spin state in BVB_2 via $SS_1 \rightarrow BVB_2$ (τ_b process) (see Supplemental Material [37]).

The spin dynamics characterized by τ_{sb} only appears at small $h\nu$ and T . It has the same sign as the dynamics characterized by τ_s ($SS_1 \rightarrow SS_2$), whereas with a similar relaxation timescale as the dynamics characterized by τ_b ($SS_1 \rightarrow BVB_2$). Such observations suggest that this dynamics might be associated with both excited SSs and bulk states, i.e., SS_2 (same sign) and BVB_2 (similar timescale). In fact, as $h\nu$ or T decreases, the non-equilibrium spin-polarized electrons excited from SS_1 to SS_2 will be at the edge of BVB_2 [Fig. 3(d)], where strong coupling between SS_2 and BVB_2 exists [43]. The energetic spin-polarized electrons can then efficiently transfer from SS_2 to available bulk states in BVB_2 , while maintaining the polarization direction as in the dynamics characterized by τ_s . This interpretation also leads to $\tau_{sb} \approx \tau_b$, as they both describe the spin relaxation of the spin-polarized electrons in BVB_2 . It naturally explains the unusual slow rise time (~ 150 fs) in the τ_{sb} process, which is needed for the charge transfer.

As an intermediate conclusion, our experiments unveil that generation of net spin polarization in three-dimensional TIs using σ^\pm photons requires the participation of the topological SSs, e.g., SS_1 and/or SS_2 in Bi_2Se_3 . Remarkably, we find that by properly tuning $h\nu$ or T , the spin-polarized electrons excited to unoccupied SSs (e.g., SS_2 in Bi_2Se_3) can have distinct spin relaxation times, depending on whether they are strongly coupled to bulk states or not. Such tunability is essential for the

development of future ultrafast spintronic devices [34]. Therefore, the underlying mechanism behind it requires to be further explored.

In a TI system such as Bi_2Se_3 , the electron spin precessing around an effective magnetic field with corresponding frequency Ω during a correlation time τ_c (average timescale of spin precession along one direction) may experience two different spin relaxation mechanisms. The first is the D'yakonov Perel' (DP) mechanism for SSs with spin-momentum locking in absence of the inversion symmetry [34]. In this case, the strong spin-orbit coupling (SOC) in SSs induces the effective magnetic field with the corresponding Ω given by the energy splitting between $E_{\vec{k}\downarrow}$ and $E_{\vec{k}\uparrow}$: $\hbar\Omega \simeq 2\hbar v_f k$ [1, 2, 34], where \vec{k} is the electron wave vector, \hbar is the reduced Planck's constant, v_f is the Fermi velocity, and $\uparrow\downarrow$ stand for spins with opposite directions. Taking $\hbar\Omega \sim 2E_f \simeq 0.2$ eV and $\tau_c \simeq \tau_p \sim 50$ fs from infrared transmission measurements [33], we thus can obtain $\Omega\tau_c \gg 1$. The second spin relaxation mechanism is the Elliot-Yafet (EY) mechanism for bulk states with inversion symmetry [34]. Here, the spin-orbit interaction, altered by phonons, causes the coupling of different spin states and leads to the spin flips via momentum scattering. The correlation time τ_c is then determined by the momentum scattering time τ_p and the inverse of the frequency f^{-1} of relevant thermal phonons [34], both of which give $\tau_c \sim 500$ fs, taking $\tau_p \sim \tau_{ep}$ and $f^{-1} \sim f^{-1}(A_{1g}^1)$. In addition, $\hbar\Omega$ can be estimated by the strength of SOC in Bi_2Se_3 , with a typical value of $\hbar\Omega \simeq \lambda_{SO} \sim 0.1$ eV [2, 44]. In fact, the coupling strength between bulk states BCB_j and BVB_j ($j = 1, 2$) can be as large as the energy gap (~ 0.3 eV) [44]. $\Omega\tau_c \gg 1$ then can also be obtained for the bulk states in EY mechanism.

The relation $\Omega\tau_c \gg 1$ implies that the electron spin precesses many full cycles during τ_c around the effective magnetic field. The spin polarization decays irreversibly after τ_c [34]. Therefore, the spin relaxation time τ^{spin} is given by $\tau^{spin} \sim \tau_c$, applied to both excited SSs and bulk states in Bi_2Se_3 , which is consistent with recent theoretical works [45–47].

Experimentally, we reveal two distinct relaxation timescales for the coherent spins excited in SSs and bulk states. The fast dynamics is characterized by $\tau_s \sim 25$ fs, which is nearly T -independent and related to the excited spin-polarized electrons in SS_2 . Since $\tau_s \sim \tau_{ep}^*$, one can conclude that the electron- E_g^2 -optical-phonon scattering dominates the scattering process in excited SS, and hence τ_s . This result is in contrast to that in the excited bulk states, where two relatively slow spin relaxation τ_b and τ_{sb} associated with BVB_2 are found to be ~ 300 fs at low T , similar to τ_{ep} ($\tau_b \simeq \tau_{sb} \sim \tau_{ep}$) [Figs. 1(b) and 2(d)]. In addition, a linear-in- T dependence is observed for τ_b^{-1} , which exactly follows the T dependence of τ_{ep}^{-1} . These observations thus suggest that the scattering/spin relaxation in excited bulk states is dominated by the A_{1g}^1

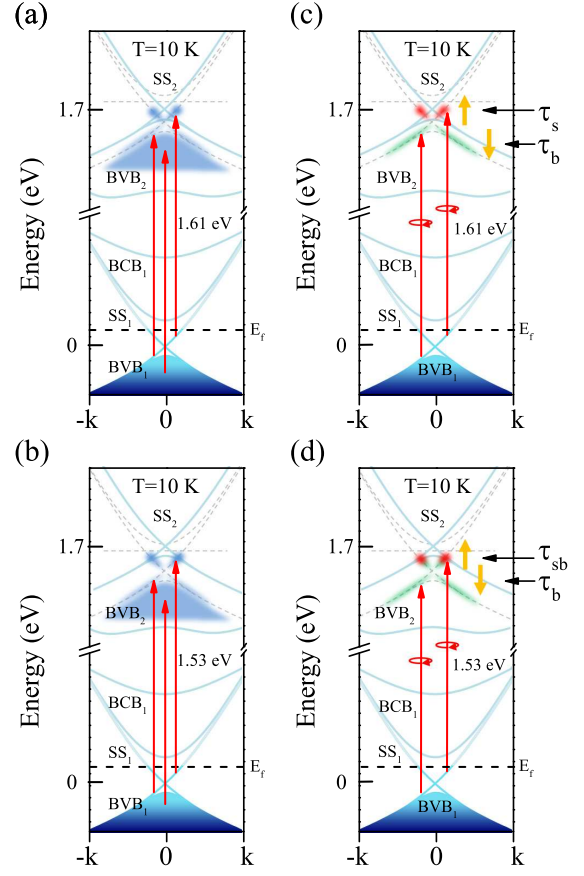


FIG. 3. Schematic illustration of the resonant photoexcitation processes in Bi_2Se_3 based on the Tr-ARPES results in Refs. [14, 19]. (a) and (b) show the electrons resonantly populated by the direct optical transitions $\text{SS}_1 \rightarrow \text{SS}_2$, $\text{SS}_1 \rightarrow \text{BVB}_2$, and $\text{BVB}_1 \rightarrow \text{BVB}_2$ (indicated by red arrows) using linearly polarized light at ~ 1.61 eV and ~ 1.53 eV, respectively. (c) and (d) show the spin-polarized electrons resonantly excited via $\text{SS}_1 \rightarrow \text{SS}_2$ (red shading) and $\text{SS}_1 \rightarrow \text{BVB}_2$ (green shading) using circularly polarized light at ~ 1.61 eV and ~ 1.53 eV, respectively. Excited electrons generated via $\text{SS}_1 \rightarrow \text{SS}_2$ in (a) and (c) are above the top of BVB_2 , and thus weakly coupled to BVB_2 . Excited electrons generated via $\text{SS}_1 \rightarrow \text{SS}_2$ in (b) and (d) are at the edge of BVB_2 , where SS_2 and BVB_2 are strongly coupled. The spin-polarized electrons generated via $\text{SS}_1 \rightarrow \text{SS}_2$ have an opposite polarization direction to that via $\text{SS}_1 \rightarrow \text{BVB}_2$ (indicated by up and down yellow arrows). In (d), the spin-polarized electrons are expected to transfer from SS_2 into BVB_2 , and thus exhibit a spin relaxation $\tau_{sb} \simeq \tau_b$, being distinct from τ_s . In all panels, black dashed lines represent the Fermi level E_f . The upper dashed lines are guides to the eye for projection of the initial states to ~ 1.61 eV or ~ 1.53 eV higher in energy. Because the electrons generated via $\text{BVB}_1 \rightarrow \text{BVB}_2$ in (a) and (b) are essentially unpolarized, they are not shown in (c) and (d).

phonon mode. Since the E_g^2 and A_{1g}^1 phonon modes have distinct energies, the spin dynamics in topological SSs and bulk states exhibit different behavior. This finding, along with previous works [20, 48–50], may inspire further investigation on dynamical properties in topological SSs.

In summary, we performed ultrafast optical spectroscopy study of spin dynamics in TI Bi_2Se_3 . We unravel that non-equilibrium net spin polarization induced by σ^\pm photons requires the participation of topological surface states (SSs) in the interband transitions. For the first time, we demonstrate that besides manipulating non-equilibrium electron spins in TI Bi_2Se_3 by switching circular polarization, one can selectively excite spin-polarized electrons to unoccupied SS_2 with two distinct spin relaxation times by only tuning the photon energy or temperature. We reveal that the distinct spin relaxation arise from the scattering in SSs and bulk states which is dominated by E_g^2 and A_{1g}^1 phonon modes, respectively. Our measurements thus pave a way to manipulate the photoinduced coherent spins in TIs, which may have profound implications in future TI-based ultrafast spintronic devices.

We would like to thank Hongming Weng and Yan Li for helpful discussions. This work was supported by China 1000-Young Talents Plan, National Natural Science Foundation of China (Grants Nos. 10979021, 11027401, 11174054, 11304338 and 11227902), the Ministry of Science and Technology of China (National Basic Research Program Grant No. 2011CB921800), the Strategic Priority Research Program (B) of the Chinese Academy of Sciences (Grant No. XDB04010100) and Helmholtz Association through the Virtual Institute for Topological Insulators (VITI). Z. Jiang acknowledges the support from the U.S. Department of Energy (Grant No. DE-FG02-07ER46451).

* jqj@pims.ac.cn

- [1] M. Z. Hasan and C. L. Kane, *Rev. Mod. Phys.* **82**, 3045 (2010).
- [2] X.-L. Qi and S.-C. Zhang, *Rev. Mod. Phys.* **83**, 1057 (2011).
- [3] W. -K Tse and A. H. MacDonald, *Phys. Rev. Lett.* **105**, 057401 (2010).
- [4] R. Valdes Aguilar et al., *Phys. Rev. Lett.* **108**, 087403 (2012).
- [5] J. I. Inoue and A. Tanaka, *Phys. Rev. Lett.* **105**, 017401 (2010).
- [6] N. H. Lindner, G. Refael, and V. Galitski, *Nature Phys.* **7**, 490 (2011).
- [7] Y. H. Wang, H. Steinberg, P. Jarillo-Herrero and N. Gedik *Science* **342**, 453 (2013).
- [8] J. W. McIver, D. Hsieh, H. Steinberg, P. Jarillo-Herrero, and N. Gedik, *Nat. Nanotechnol.* **7**, 96 (2011).
- [9] H. Z. Lu, W. Y. Shan, W. Yao, Q. Niu, and S. Q. Shen, *Phys. Rev. B* **81**, 115407 (2010).
- [10] P. Hosur, *Phys. Rev. B* **83**, 035309 (2011).
- [11] A. Junck, G. Refael, and F. von Oppen, *Phys. Rev. B* **88**, 075144 (2013).
- [12] C. Kastl, C. Karnetzky, H. Karl, and A. W. Holleitner, *Nat. Comm.* **6**, 6617 (2015).
- [13] D. Pesin and A. H. Macdonald, *Nat. Mater.* **11**, 409 (2012).
- [14] J. A. Sobota et al., *Phys. Rev. Lett.* **108**, 117403 (2012).
- [15] Y. H. Wang et al., *Phys. Rev. Lett.* **109**, 127401 (2012).
- [16] M. Hajlaoui et al., *Nano Lett.* **12**, 3532 (2012).
- [17] A. Crepaldi et al., *Phys. Rev. B* **86**, 205133 (2012).
- [18] J. A. Sobota et al., *Phys. Rev. Lett.* **111**, 136802 (2013).
- [19] J. A. Sobota et al., *J. Electron Spectrosc. Relat. Phenom.* **149**, 295 (2014).
- [20] J. A. Sobota et al., *Phys. Rev. Lett.* **113**, 157401 (2014).
- [21] C. Cacho et al., *Phys. Rev. Lett.* **114**, 097401 (2015).
- [22] J. Qi et al., *Appl. Phys. Lett.* **97**, 182102 (2010).
- [23] N. Kumar et al., *Phys. Rev. B* **83**, 235306 (2011).
- [24] D. Hsieh et al., *Phys. Rev. Lett.* **107**, 077401 (2011).
- [25] H.-J. Chen et al., *Appl. Phys. Lett.* **101**, 121912 (2012).
- [26] Y. D. Glinka et al., *Appl. Phys. Lett.* **103**, 151903 (2013).
- [27] C. W. Luo et al., *Nano Lett.* **13**, 5797 (2013).
- [28] Y. Lai, H. Chen, K. Wu, and J. Liu, *Appl. Phys. Lett.* **105**, 232110 (2014).
- [29] L. Cheng et al., *Appl. Phys. Lett.* **104**, 211906 (2014).
- [30] S. Sim et al., *Phys. Rev. B* **89**, 165137 (2014).
- [31] R. V. Aguilar et al., *Appl. Phys. Lett.* **106**, 011901 (2015).
- [32] Y. Onishi et al., *Phys. Rev. B* **91**, 085306 (2015).
- [33] N. P. Butch et al., *Phys. Rev. B* **81**, 241301 (2010).
- [34] I. Zutic, J. Fabian, and S. D. Sarma, *Rev. Mod. Phys.* **76**, 323 (2004); M. W. Wu, J. H. Jiang, and M. Q. Weng, *Phys. Rep.* **493**, 61236 (2010); M. I. D'yakonov, ed., *Spin Physics in Semiconductors* (Springer-Verlag Berlin Heidelberg, 2008).
- [35] J. Sanchez-Barriga et al., arXiv:1505.02742.
- [36] F. Boschini et al., arXiv:1506.02692.
- [37] See Supplemental Material, which includes Refs.[51–57].
- [38] G. A. Garret, T. F. Albrecht, J. F. Whitaker, and R. Merlin, *Phys. Rev. Lett.* **77**, 3661 (1996); R. Merlin, *Solid State Comm.*, **102**, 207 (1997).
- [39] T. K. Cheng et al., *Appl. Phys. Lett.* **59**, 1923 (1991).
- [40] W. Richter, H. Kohler, and C. R. Becker, *phys. stat. sol. (b)* **6**, 619 (1977)
- [41] F. Meier and B. P. Zakharchenya, eds., *Optical Orientation* (Elsevier, Amsterdam,1984).
- [42] M. Cardona and M. L. W. Thewalt, *Rev. Mod. Phys.* **77**, 1173 (2005).
- [43] O. V. Yazyev, J. E. Moore, and S. G. Louie, *Phys. Rev. Lett.* **105**, 266806 (2010).
- [44] C. X. Liu et al., *Phys. Rev. B* **82**, 045122 (2010).
- [45] A. A. Burkov and D. G. Hawthorn, *Phys. Rev. Lett.* **105**, 066802 (2010).
- [46] X. Liu, and J. Sinova, *Phys. Rev. Lett.* **111**, 166801 (2013).
- [47] P. Zhang and M. W. Wu, *Phys. Rev. B* **87**, 085319 (2013).
- [48] X. Zhu et al., *Phys. Rev. Lett.* **107**, 186102 (2011).
- [49] X. Zhu et al., *Phys. Rev. Lett.* **108**, 185501 (2012).
- [50] M. V. Costache et al., *Phys. Rev. Lett.* **112**, 086601 (2014).
- [51] J. Qi et al., *Phys. Rev. B* **79**, 085304 (2009).
- [52] J. Qi et al., *Phys. Rev. Lett.* **111**, 057402 (2013).
- [53] Y. Kim et al., *Appl. Phys. Lett.* **100**, 071907 (2012).
- [54] X. Chen et al., *Appl. Phys. Lett.* **99**, 261912 (2011).
- [55] H. M. Benia, C. Lin, K. Kern, and C. R. Ast, *Phys. Rev. Lett.* **107**, 177602 (2011).
- [56] P. D. C. King et al., *Phys. Rev. Lett.* **107**, 096802 (2011).
- [57] D. J. Hilton and C. L. Tang, *Phys. Rev. Lett.* **89**, 146601 (2002).